

High-efficiency transparent organic light-emitting devices

Parthasarathy, G.

Center for Photonics and Optoelectronic Materials (POEM), Department of Electrical Engineering and the Princeton Materials Institute, Princeton University

Adachi, Chihaya

Center for Photonics and Optoelectronic Materials (POEM), Department of Electrical Engineering and the Princeton Materials Institute, Princeton University

Burrows, P.E.

Center for Photonics and Optoelectronic Materials (POEM), Department of Electrical Engineering and the Princeton Materials Institute, Princeton University

Forrest, Stephen R.

Center for Photonics and Optoelectronic Materials (POEM), Department of Electrical Engineering and the Princeton Materials Institute, Princeton University

<https://hdl.handle.net/2324/19446>

出版情報 : Applied Physics Letters. 76 (15), pp.2128-2130, 2000-04-10. American Institute of Physics

バージョン :

権利関係 : Copyright 2000 American Institute of Physics. This article may be downloaded for personal use only. Any other use requires prior permission of the author and the American Institute of Physics.



High-efficiency transparent organic light-emitting devices

G. Parthasarathy, C. Adachi, P. E. Burrows, and S. R. Forrest^{a)}

Center for Photonics and Optoelectronic Materials (POEM), Department of Electrical Engineering, and Princeton Materials Institute (PMI), Princeton University, Princeton, New Jersey 08544

(Received 20 January 2000; accepted for publication 14 February 2000)

We demonstrate organic light-emitting devices (OLEDs) employing highly transparent cathodes comprised of 2,9-dimethyl-4,7 diphenyl-1,10-phenanthroline (BCP) and an ultrathin film of Li capped with radio-frequency magnetron-sputtered indium–tin–oxide. The cathodes are incorporated onto a conventional bilayer small-molecule OLED. The operating voltages and the total device external quantum efficiencies emitted from the top and substrate surfaces ($1.0 \pm 0.05\%$) are comparable to the best conventional undoped OLEDs employing thick metallic cathodes. The device characteristics are independent of the position of Li within the compound cathode, suggesting that Li readily diffuses through BCP to enhance electron injection. An increase of a factor ~ 3.5 in the external quantum efficiency is observed compared to devices containing no Li. These results suggest that Li donates electrons to the BCP, increasing its conductivity to the point that band bending occurs to aid in the injection of charge. © 2000 American Institute of Physics. [S0003-6951(00)05015-4]

Applications of transparent cathodes for organic thin-film devices include organic light emitters (OLEDs) integrated with either Si or organic thin-film transistor driver electronics for active-matrix displays and low-optical-loss contacts for electrically pumped organic solid-state lasers.^{1–4} Previously, such transparent cathodes were deposited by radio-frequency sputtering of indium–tin–oxide (ITO) on top of a thin (~ 100 Å) semitransparent metal film such as Mg:Ag. However, the total external quantum efficiencies of these devices are approximately half that of conventional OLEDs, and their transparency is limited to $\leq 70\%$ in the visible.^{5,6} Recently, a more transparent, although somewhat less efficient metal-free cathode was introduced employing a thin layer of copper phthalocyanine (CuPc) in place of the semitransparent metal film.⁷ The external quantum efficiency (η) of these metal-free devices was recently improved to $\eta \sim 0.75\%$, or nearly that of a conventional OLED employing a thick metal cathode by the insertion of a thin (~ 3 Å) film of Li *between* the CuPc and the ITO.⁸ In this work, we show that by replacing the CuPc with 2,9-dimethyl-4,7 diphenyl-1,10-phenanthroline (BCP) and inserting a thin film (~ 5 – 10 Å) of Li *anywhere* within the compound cathode structure, we can achieve a total external quantum efficiency of $(1.0 \pm 0.05)\%$ at a drive current of 10 mA/cm^2 , with a transparency of $\sim 90\%$ across the entire visible spectrum. These results suggest that Li readily diffuses throughout the BCP and acts as an electron donor, creating a highly doped degenerate surface layer to enhance electron injection into the OLED.

We fabricated four sets of transparent metal-free OLEDs on precleaned and ultraviolet-ozone-treated⁹ ITO-coated glass substrates. First, 650 Å of the hole-transporting layer 4,4-bis[*N*-(1-naphthyl)-*N*-phenyl-amino] biphenyl (α -NPD) was vacuum (base pressure of 10^{-7} Torr) deposited on the ITO, followed by 750 Å of the emissive, electron-transporting layer: tris-(8-hydroxyquinoline) aluminum

(Alq₃). A 1500 -Å-thick Mg:Ag (10:1 mass ratio) cathode followed by a 500 Å cap of Ag was then deposited onto the Alq₃ surface through a shadow mask to form the conventional, control OLEDs. The three other sets of devices employed the following cathode variations: (a) ITO/BCP; (b) ITO/BCP/Li; and (c) ITO/Li/BCP. The thickness of the ITO was 525 Å, the BCP was 70 Å, and the Li was 5 – 10 Å. The ITO was radio-frequency magnetron sputtered from a 10 -cm-diam target at a power of 50 W, an Ar flow rate of 140 sccm, and a pressure of 2 mTorr,⁶ yielding a deposition rate of 0.3 Å/s. Elemental Li in the form of a rod¹⁰ was thermally evaporated at a rate of 1 Å/s. All transparent devices were fabricated without a vacuum break.

The four sets of devices have similar current density–voltage (J – V) characteristics (Fig. 1) showing two distinct regimes of transport characteristics of small-molecule OLEDs:¹¹ Ohmic transport at low-drive voltages following $J \sim V$, and trapped-charge-limited transport at higher-drive

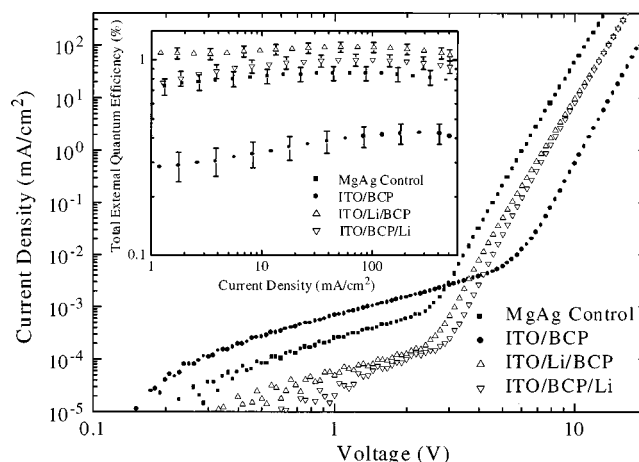


FIG. 1. Current density vs voltage (J – V) plot of OLEDs with the following structure: cathode/Alq₃/α-NPD/ITO where the cathode is Mg:Ag, ITO/BCP, ITO/Li/BCP, and ITO/BCP/Li. Inset: total external quantum efficiency (η) vs current density (J) for the four devices in Fig. 1.

^{a)}Electronic mail: forrest@ee.princeton.edu

voltages following $J \sim V$.⁹ The “operating voltage” is obtained at a current density of 10 mA/cm² corresponding to a luminance of ~ 100 cd/m², the nominal requirement for video applications. Both the Li-containing and Mg:Ag contact devices have similar operating voltages of ~ 9 V (to within 1 V). However, the conventional metal-free device without Li shows a marked increase to 14.5 V due to the large injection barrier at the ITO/BCP interface. In all cases, the low-voltage regime shows a very low-leakage current density of $\leq 10^{-5}$ A/cm², although the Li-free devices had a somewhat higher leakage. Yield, defined as the ratio of non-shorted to the total number of devices tested, for each of the four sets of devices was 100% for a sample size of 16.

The total external quantum efficiencies of the devices are plotted in the inset of Fig. 1. For the transparent devices, the optical output power is the sum of that emitted from both the substrate and the cathode surfaces.⁷ At $J = 10$ mA/cm², the OLED with the metallic cathode has $\eta = (0.85 \pm 0.05)\%$ while the transparent devices containing Li have $\eta = (1.0 \pm 0.05)\%$. However, the transparent device without Li shows $\eta = (0.30 \pm 0.05)\%$, consistent with previous results.⁷ Again, this is presumed to be due to the large barrier to electrons at the cathode, leading to imbalanced injection of charge, and thus a lower η .

As previously,⁸ the insertion of 5–10 Å of Li improves the external quantum efficiency of metal-free OLEDs. Our experiments show that inserting a thicker Li layer results in a decrease of η , ultimately eliminating the benefits introduced with the very thin layers discussed here.¹² In addition, by using BCP instead of CuPc in the cathode, we have shown a $\sim 40\%$ increase in the external quantum efficiency. To make these cathodes useful for integration in full-color displays, it is necessary to have high transparency across the entire visible spectrum, thus further motivating the use of a $\sim 90\%$ transparent BCP/Li cathode instead of CuPc/Li, the latter cathodes being only 65%–85% transparent in the visible.¹³

To understand the losses incurred when using CuPc instead of BCP beneath the ITO contact, we measured the relative photoluminescence (PL) efficiencies of the following structures all grown on quartz: (i) Alq₃; (ii) ITO/BCP/Alq₃; (iii) ITO/CuPc/Alq₃; and (iv) ITO/Alq₃. The thickness of the Alq₃ was 100 Å, the CuPc and BCP were 70 Å, and the ITO cap was 525 Å. A mercury lamp in conjunction with a 10-nm-wide optical bandpass filter centered at the wavelength of $\lambda = 400$ nm was used as the excitation source incident via the quartz substrate, creating excitons uniformly throughout the Alq₃ layer.¹¹ Further, CuPc is nearly transparent at $\lambda = 400$ nm,⁷ eliminating effects due to exciton generation in that layer. Figure 2 shows that the ratio of the PL efficiencies for structures (i):(ii):(iii):(iv) are 16:10:1:1. Since the thicknesses of the organic layers and the ITO were kept constant, microcavity effects do not play a significant role in determining the shape or intensity of the PL spectra in Fig. 2.⁹ We conclude, therefore, that BCP prevents the dramatic quenching of Alq₃ excitons due to the sputter-induced damage from the ITO at the cathode.^{3,7} As in past reports,³ BCP acts effectively in blocking exciton transport to the damaged ITO/organic interface. In contrast, CuPc does not appear to significantly re-

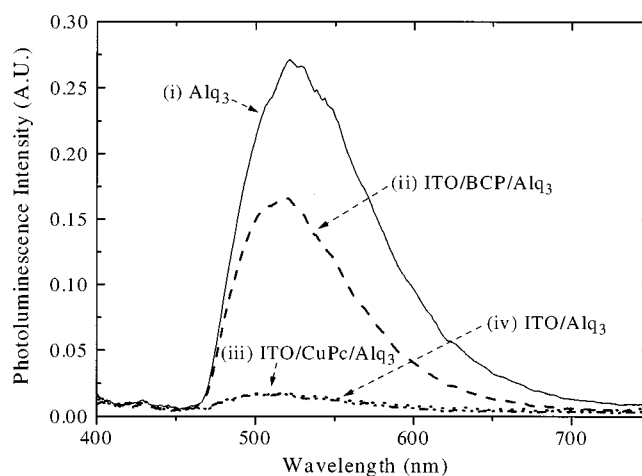


FIG. 2. Photoluminescence intensity vs wavelength of the following structures grown on quartz: (i) Alq₃; (ii) ITO/BCP/Alq₃; (iii) ITO/CuPc/Alq₃; and (iv) ITO/Alq₃.

duce quenching compared to that observed by direct deposition of ITO onto Alq₃.

To separate the quenching of Alq₃ emission due to the presence of CuPc from that due to the sputter damage under the ITO, the following second set of structures was grown on quartz with the same thicknesses as above: (i) Alq₃; (ii) BCP/Alq₃; (iii) CuPc/BCP/Alq₃; and (iv) CuPc/Alq₃. The ratio of the PL efficiencies for structures (i):(ii):(iii):(iv) are 12:10:6:1, as shown in Fig. 3. This shows that CuPc itself quenches Alq₃ emission, possibly via exciplex formation at the organic heterointerface. In addition, these experiments indicate that BCP, previously shown to be a barrier to Alq₃ exciton transport, can be placed between CuPc and Alq₃ to partially recover the Alq₃ PL intensity by preventing excitons from migrating to the damaged region immediately below the sputtered ITO contact.

It is known that Li diffuses through organics,^{14,15} and thus it is not surprising that placing Li on either side of the BCP layer makes no significant difference in the device characteristics. However, it was reported that the insertion of Li

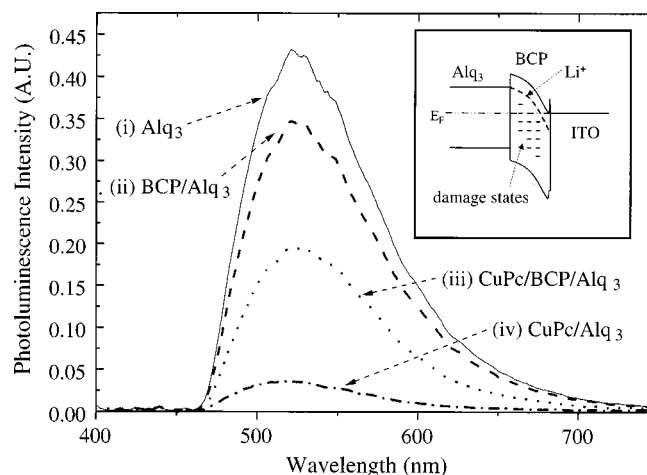


FIG. 3. Photoluminescence intensity vs wavelength of the following structures grown on quartz: (i) Alq₃; (ii) BCP/Alq₃; (iii) CuPc/BCP/Alq₃; and (iv) CuPc/Alq₃. Inset: proposed energy-level diagram of the degenerately doped BCP/Li⁺ layer referenced to the Fermi level (E_F) at thermal equilibrium. The damage states are due to ITO deposition, and assist in efficient electron injection.

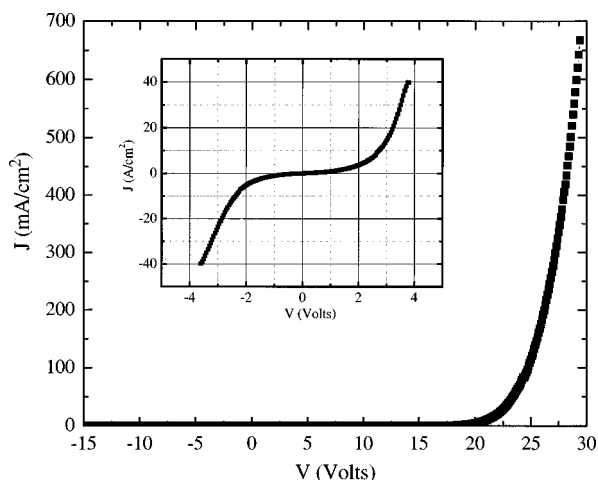


FIG. 4. Current density vs voltage (J - V) characteristics of a Ag/BCP/ITO device. Inset: J - V characteristics of the same device in Fig. 4 with the addition of ~ 10 Å of Li at the Ag/BCP interface.

between CuPc and Alq₃ resulted in a substantial increase in the operating voltage when compared to inserting Li between CuPc and the ITO cap.⁸ We have not observed this discrepancy with the CuPc/Li system, and attribute the apparent discrepancy to differences in the fabrication process of the top ITO contact.¹³

Our data, combined with the fact that Li acts to improve electron injection,¹⁶ suggests that Li dopes the BCP layer by donating its valence electron, thereby forming Li⁺. This results in band bending, making it easier to inject charge from the ITO contact into the bulk of the Alq₃. Assuming a bulk density of 0.53 g/cm³, 10 Å of Li can donate up to 10^{16} cm⁻² electrons into the ~ 100 -Å-thick BCP layer, leading to an electron density of $\sim 10^{21}$ cm⁻³. At these densities the BCP is a degenerate semiconductor which establishes an Ohmic contact with the bulk organic semiconductor (see the inset, Fig. 3). By depositing a thicker continuous layer of Li, the Li atoms are tied to the surface, consequently, reducing both diffusion and doping. This explains why Li thicknesses ≥ 10 Å are ineffective in producing high-efficiency OLEDs.

To test the hypothesis of Li⁺ diffusion and doping, structures of the form: 1500 Å Ag/800 Å BCP/ITO were fabricated with and without ~ 10 Å Li at the Ag/BCP interface. As shown in Fig. 4, the Li-free device has a rectification ratio of $\sim 10^5$ measured at ± 30 V. In contrast, the device containing ~ 10 Å of Li between the BCP and the Ag shows nearly Ohmic behavior at low V , with a contact resistance of ~ 1 Ω cm². This allows for very large current den-

sities (~ 40 A/cm²) at low voltages (~ 2 V) with a rectification ratio of ~ 1 at ± 3.5 V. We infer from these data that Li diffuses throughout the 800 Å BCP layer,¹⁵ degenerately doping the BCP to yield a highly conductive layer enabling efficient electron injection.

In conclusion, we have fabricated high-efficiency, high-transparency organic light-emitting devices using a compound ITO/BCP/Li cathode whose device characteristics are similar to conventional OLEDs employing thick metal cathodes. The replacement of CuPc with BCP also increases the overall transparency of the devices to $\sim 90\%$ across the visible spectrum. Photoluminescence experiments have shown that BCP efficiently blocks excitons and prevents ITO sputter-induced damage of the underlying organic layers from significantly quenching the luminescence. These data further suggest that Li diffuses through BCP and acts as a donor of free electrons into the BCP conduction level. Degenerate doping leads to band bending, further facilitating efficient electron injection from the ITO contact into the underlying organic layers comprising the OLED.

The authors thank S. Mao for technical assistance and Professor M. E. Thompson for useful discussions. The authors are also grateful to DARPA, the Universal Display Corporation, and AFOSR for their generous support of this research.

¹R. F. Service, *Science* **273**, 878 (1996).

²V. G. Kozlov, G. Parthasarathy, V. B. Khalfin, J. Wang, S. Y. Chou, and S. R. Forrest, *IEEE J. Quantum Electron.* **36**, 18 (2000).

³G. Parthasarathy, G. Gu, and S. R. Forrest, *Adv. Mater.* **11**, 907 (1999).

⁴A. Dodabalapur, Z. Bao, A. Makhija, J. G. Laquidant, V. R. Raju, Y. Feng, H. E. Katz, and J. Rogers, *Appl. Phys. Lett.* **73**, 142 (1998).

⁵G. Gu, V. Bulovic, P. E. Burrows, S. R. Forrest, and M. E. Thompson, *Appl. Phys. Lett.* **68**, 2606 (1996).

⁶P. E. Burrows, G. Gu, E. P. Vicenzi, S. R. Forrest, and T. X. Zhou, *J. Appl. Phys.* **87**, 3080 (2000).

⁷G. Parthasarathy, P. E. Burrows, V. Khalfin, V. G. Kozlov, and S. R. Forrest, *Appl. Phys. Lett.* **72**, 2138 (1998).

⁸L. S. Hung and C. W. Tang, *Appl. Phys. Lett.* **74**, 3209 (1999).

⁹G. Gu, G. Parthasarathy, P. E. Burrows, P. Tian, I. G. Hill, A. Kahn, and S. R. Forrest, *J. Appl. Phys.* **86**, 4067 (1999).

¹⁰Elemental Li was purchased from Alfa Aesar, Ward Hill, MA.

¹¹P. E. Burrows, Z. Shen, V. Bulovic, D. M. McCarty, S. R. Forrest, J. A. Cronin, and M. E. Thompson, *J. Appl. Phys.* **79**, 7991 (1996).

¹²C. W. Tang (private communication).

¹³G. Parthasarathy and S. R. Forrest (unpublished results).

¹⁴E. I. Haskal, A. Curioni, P. F. Seidler, and W. Andreoni, *Appl. Phys. Lett.* **68**, 2606 (1997).

¹⁵N. Johansson, T. Osada, S. Stafstrom, W. R. Salaneck, V. Parente, D. A. dos Santos, X. Crispin, and J. L. Bredas, *J. Chem. Phys.* **111**, 2157 (1999).

¹⁶J. Kido and T. Matsumoto, *Appl. Phys. Lett.* **73**, 2866 (1998).